IEEE Access
Multidisciplinary | Rapid Review | Open Access Journal

Received 23 October 2023, accepted 14 November 2023, date of publication 16 November 2023,
date of current version 22 November 2023.

Digital Object Identifier 10.1109/ACCESS.2023.3334167

RESEARCH ARTICLE

N-Ary Alamouti Space-Time Block Coding With and Without Golden Codewords

HONGJUN XU[1], (Member, IEEE), NARUSHAN PILLAY[1], AND FENGFAN YANG[2]
[1]School of Engineering, University of KwaZulu-Natal, Durban 4041, South Africa
[2]College of Electronic and Information Engineering, Nanjing University of Aeronautics and Astronautics (NUAA), Nanjing 210016, China
Corresponding author: Narushan Pillay (pillayn@ukzn.ac.za)

ABSTRACT Information is conveyed by either time, antenna, and/or frequency in the conventional modulation. In this paper, we propose a novel technique to convey information in Alamouti space-time block coding systems. In the proposed technique, the information can be conveyed by one channel's phase component with order N. The proposed technique is referred to as $2 \times N_r$ N-ary Alamouti-STBC (N-STBC), where N_r is the number of receive antennas. The N-STBC with Golden codewords (GCs) is further proposed to improve error performance at high signal-to-noise ratios (SNRs). Moreover, the proposed N-STBC with and without GCs still preserves the orthogonal transmission matrix of the Alamouti-STBC which retains the simple linear maximum-likelihood (L-ML) detection for quasi-static frequency-flat Rayleigh fading channels. The transmitted symbols can be directly estimated by use of the L-ML detection in the N-STBC with and without GCs. However, only the GCs are estimated by use of the L-ML detection in N-STBC with GCs. The signal detection subset based ML detection is further employed to detect the transmitted M-ary quadrature amplitue modulation (MQAM) symbols in N-STBC with GCs. The lower error probability bounds of the N-STBC with and without GCs are derived and validated by simulation results. As an example, the proposed 2×4 16QAM 16-STBC with GCs almost maintain the error performance of the conventional Alamouti-STBC with GCs at SNRs.

INDEX TERMS Bit error probability, Golden codewords, M-ary phase shift keying modulation, M-ary quadrature amplitude modulation, N-ary Alamouti space-time block coding.

I. INTRODUCTION

High data transmission rates are required in 5th generation (5G) wireless communication systems [1]. Multiple-input multiple-output (MIMO) is a key technique to meet the high data transmission rate and the very good channel reliability. One type of MIMO systems is space-time block code (STBC) system. The Alamouti space-time block code [2], hereinafter referred to as Alamouti-STBC, employs only two transmit antennas, which simultaneously transmit two message symbols over two consecutive transmission intervals. The transmission matrix maintains an orthogonal structure, which allows for simple linear maximum-likelihood (L-ML) detection in a quasi-static frequency-flat Rayleigh fading channel. Alamouti-STBC has been shown to achieve full-diversity and half-rate, while not requiring additional system resources [2], [3], [4], where the rate is defined as the number of transmitted symbols/time slots/per antenna.

Several attempts have been made to improve the spectral efficiency of Alamouti-STBC. For example, in [5], two quadrature phase shift keyed (QPSK) constellations are employed in STBC, allowing for an additional bit to be mapped to one of the constellations. Athough the scheme maintains the simple decoupled ML detector of Alamouti-STBC [2], the improvement is limited, since it is not generalized to more than two constellations. In [6], a rate-2 STBC based on field extensions was proposed for QPSK. However, the computational complexity imposed for ML detection is extremely high. In [7], a high rate STBC for QPSK was proposed, where the signal set is enlarged by considering a coset of the STBC transmission matrix. An additional bit is then mapped to one of the transmission signal sets. Optimum power scaling is further employed to ensure full-diversity; however, the achievable spectral efficiency is limited. High

The associate editor coordinating the review of this manuscript and approving it for publication was Jose Saldana.

rate embedded Alamouti-STBC (EAST) was presented in [8]. EAST can employ even numbers of transmit antennas up to 8; however, for 2 transmit antennas EAST reduces to STBC [2], hence it is only half-rate. Meanwhile, space-time block coded spatial modulation (STBC-SM) was proposed in [9]. STBC-SM combines the Alamouti-STBC with conventional SM to improve the error performance of SM by exploiting transmit diversity. In order to reduce the number of transmit antennas space-time block coded spatial modulation with cyclic structure (STBC-CSM) was proposed in [10]. Further cyclic temporally and spatially-modulated STBC (STBC-TSM) was proposed in [11]. STBC-TSM can further reduce error rate compared to STBC-SM and STBC-CSM. However, in the case of [9], [10], and [11], although only two transmit antennas are active per transmission interval more than two transmit antennas are required to facilitate the mapping of additional bits. Furthermore, these schemes exploit the concept of spatially modulated transmission [9], [10], [11], hence being quite different from the Alamouti-STBC.

In this paper, we also focus on the Alamouti-STBC based transmission scheme with two transmit antennas to improve spectral efficiency and approximately retain the bit error performance as the conventional Alamouti-STBC. In this paper, we propose a novel technique to convey information in the Alamouti-STBC systems, which is referred to as N-ary Alamouti-STBC (N-STBC). The proposed N-STBC needs two consecutive Alamouti-STBC block transmissions. Compared to the conventional Alamouti-STBC, the extra information is conveyed by one pair of coupled phase offsets to the signal transmitted through one of the two transmit antennas during two consecutive block transmissions in the proposed N-STBC system. Given $\log_2 N$ bits which are mapped to one pair of N-ary phase shift keying (NPSK) space-time labelling diversity (STLD) signals [12], $(e^{j\theta_p^1}, e^{j\theta_p^2}), e^{j\theta_p^l}$ will be applied in l block transmission.

Space shift keying (SSK) is a spatial modulation based new modulation [13]. In SSK there are more than one transmit antennas. But only one transmit antenna is active during transmission. During transmission only the transmit antenna index conveys information. The transmitted symbol does not convey any information. Compared to SSK the proposed N-ary Alamouti-STBC only contains two transmit antennas. During transmission two transmit antennas are all active. Both the transmitted symbols and one pair of NPSK STLD signals convey information.

In order to achieve more diversity Golden codewords (GCs) have been applied in single-input multiple-output (SIMO) systems in [14], reconfiguration intelligent surface-aided SIMO system in [15] and space-time line code system in [16]. Motivated by the work in [14], [15], and [16], the N-STBC with GCs has also been proposed in this paper. Compared to the N-STBC without GCs, the N-STBC with GCs achieves $4N_r$ diversity order, and further improve error performance at high signal-to-noise ratios (SNRs).

The proposed technique, the N-STBC with and without GCs, involves an additional pair of coupled phase components in the transmission at one of two transmit antennas. Additional information bits are then mapped to one pair of the coupled phase components, which has N degrees-of-freedom. No additional power or bandwidth is required for the proposed technique. Furthermore, the proposed N-STBC with and without GCs still keeps the orthogonal transmission matrix of the Alamouti-STBC which retains the simple L-ML detection for quasi-static frequency-flat Rayleigh fading channels.

In the proposed N-STBC with GCs, the GCs not the M-ary quadrature amplitude modulation (MQAM) or MPSK symbols, are estimated by use of the L-ML detection. The signal detection subset based ML detection (SDS-ML) proposed in [14] is further employed to detect the transmitted MQAM symbols to improve error performance at high SNRs.

The main contributions of this paper are:

Contribution 1: This paper proposes a novel transmission technique in the Alamouti-STBC systems, the N-STBC with and without GCs.

Contribution 2: This paper derives lower error probability bounds of the proposed N-STBC with and without GCs.

The remainder of the paper is organized as follows: Preliminary concepts of the STLD and Golden code are introduced in Section II. In Section III, the system model is presented. Signal detections for the N-STBC with and without GCs are presented in Section IV. Lower error probability bounds of the N-STBC with and without GCs are derived in Section V. In Section VI, the numerical results are demonstrated. Finally, the paper is concluded in Section VII.

Notation: Bold lowercase and uppercase letters are used for vectors and matrices, respectively. $[\cdot]^T$, $(\cdot)^H$, $|\cdot|$ and $\|\cdot\|_F$ represent the transpose, Hermitian, Euclidean and Frobenius norm operations, respectively. $\mathcal{D}(\cdot)$ is the constellation demodulator function. $E\{\cdot\}$ is the expectation operation. $j = \sqrt{-1}$ is a complex number. Finally $\langle , \rangle$ denotes the inner product operation.

II. PRELIMINARY CONCEPTS

Both STLD and Golden code are key components in the proposed system. In this section, as preliminaries, we briefly present the STLD and Golden code.

A. SPACE-TIME LABELLING DIVERSITY (STLD)

STLD is an STBC with two transmit antennas. Consider an $N_t \times N_r$ conventional STLD system, where N_t and N_r are the numbers of transmit and receive antennas ($N_t = 2$, and $N_r \geq N_t$). In the conventional STLD system, there are two input information bit streams, $\boldsymbol{b}_i, i \in [1:2]$, and two bit-to-symbol mappers, $\Omega_M^k, k \in [1:2]$. Normally, Ω_M^1 is the Gray coded mapper, while Ω_M^2 is designed for a specific modulation scheme [12]. Let $\boldsymbol{\chi}_M$ be the signal set of MQAM or MPSK. In order to achieve labelling diversty $M \geq 8$. Let the two input information bit streams be $\boldsymbol{b}_i = [b_{i,1} \cdots b_{i,r}]$, $i \in [1:2]$, $r = \log_2 M$, where M is the order of MQAM or MPSK modulation. Then bit stream $\boldsymbol{b}_i$ is fed into Ω_M^k, which maps the r input bits onto constellation points

from $\boldsymbol{\chi}_M$, and yields the symbols, $x^k_{\boldsymbol{b}_i} = \Omega^k_M(\boldsymbol{b}_i)$, $k \in [1:2]$, where $E\{|x^k_{\boldsymbol{b}_i}|^2\} = 1$.

The codeword matrix of the STLD is given by [12]:

$$\boldsymbol{X}_L = \begin{bmatrix} x^1_{\boldsymbol{b}_1} & x^2_{\boldsymbol{b}_2} \\ x^1_{\boldsymbol{b}_2} & x^2_{\boldsymbol{b}_1} \end{bmatrix}. \tag{1}$$

In the STLD system, transmit antennas 1 and 2 transmit, respectively, $x^1_{\boldsymbol{b}_1}$ and $x^2_{\boldsymbol{b}_2}$ in time slot 1, and $x^1_{\boldsymbol{b}_2}$ and $x^2_{\boldsymbol{b}_1}$ in time slot 2. Since two information bit streams are transmitted in two time slots using two transmit antennas, the STLD has only half-rate. However, the STLD not only achieves full-diversity, but also achieves labelling diversity [12].

There are two pairs of MQAM or MPSK symbols, $(x^1_{\boldsymbol{b}_1}, x^2_{\boldsymbol{b}_1})$ and $(x^1_{\boldsymbol{b}_2}, x^2_{\boldsymbol{b}_2})$, in the STLD system. The STLD system has two key behaviors. One is that both $x^1_{\boldsymbol{b}_i}$ and $x^2_{\boldsymbol{b}_i}$ in each pair $(x^1_{\boldsymbol{b}_i}, x^2_{\boldsymbol{b}_i})$ convey the same information. The other is that the error performance of the STLD system mainly depends on the minimum product Euclidean distance [12], which is determined by two bit-to-symbol mappers. The first mapper is Gray mapper which is given. We only need to design the second mapper. The objective of designing the second mapper Ω^2_M is to maximize the minimum product Euclidean distance, which is a massive combinatorial problem [12]. In this paper, only one pair of NPSK STLD symbols is used in the proposed N-STBC technique. As an example, the two mappers for one pair of 16PSK STLD shown in Fig. 1 in [12] is also tabulated in TABLE 1 in this paper.

TABLE 1. Constellation mappers for 16PSK.

q	0	1	2	3	4	5	6	7
Ω^1_{16}	θ_0	θ_1	θ_3	θ_2	θ_7	θ_6	θ_4	θ_5
Ω^2_{16}	θ_0	θ_9	θ_{11}	θ_2	θ_{15}	θ_6	θ_4	θ_{13}
q	8	9	10	11	12	13	14	15
Ω^1_{16}	θ_{15}	θ_{14}	θ_{12}	θ_{13}	θ_8	θ_9	θ_{11}	θ_{10}
Ω^2_{16}	θ_7	θ_{14}	θ_{12}	θ_5	θ_8	θ_1	θ_3	θ_{10}

In TABLE 1, q stands for the corresponding decimal index of the input information bits and θ_x denotes for $e^{j\frac{2\pi}{16}\times x}$. Suppose that the input information bits are 0100 then $q = 4$ and the pair of 16PSK STLD symbols is $(e^{j\frac{2\pi}{16}\times 7}, e^{j\frac{2\pi}{16}\times 15})$. Designing the second mapper in TABLE 1 is solved by a heuristic approach [12]. Similarly we also use the heuristic approach to design the second mapper for 8PSK and 32PSK. The two mappers of 8PSK and 32PSK are tabulated in TABLEs 2 and 3 in Appendix A.

B. THE GOLDEN CODE AND THE GOLDEN CODEWORDS

The Golden code is a linear dispersion space-time block code (LD-STBC) with two transmit antennas and two or more receive antennas [17]. The Golden code achieves full rate and full diversity. The Golden encoder takes four complex-valued symbols x_i, and generates four super-symbols. The Golden codeword matrix is given by [17]:

$$\boldsymbol{X}_G = \begin{bmatrix} \frac{1}{\sqrt{5}}\alpha(x_1 + x_2\theta) & \frac{1}{\sqrt{5}}\alpha(x_3 + x_4\theta) \\ \frac{1}{\sqrt{5}}j\bar{\alpha}(x_3 + x_4\bar{\theta}) & \frac{1}{\sqrt{5}}\bar{\alpha}(x_1 + x_2\bar{\theta}) \end{bmatrix}. \tag{2}$$

where $\theta = \frac{1+\sqrt{5}}{2}$, $\bar{\theta} = 1 - \theta$, $\alpha = 1 + j\bar{\theta}$, and $\bar{\alpha} = 1 + j\theta$. Note $x_i \in \boldsymbol{\chi}_M$.

In (2), there are four super-symbols, $\frac{1}{\sqrt{5}}\alpha(x_1 + x_2\theta)$, $\frac{1}{\sqrt{5}}\bar{\alpha}(x_1 + x_2\bar{\theta})$, $\frac{1}{\sqrt{5}}\alpha(x_3 + x_4\theta)$ and $\frac{1}{\sqrt{5}}j\bar{\alpha}(x_3 + x_4\bar{\theta})$. In this paper, we refer to these super-symbols as the Golden codewords (GCs). There are two pairs of GCs, $\left\{\frac{1}{\sqrt{5}}\alpha(x_1 + x_2\theta), \frac{1}{\sqrt{5}}\bar{\alpha}(x_1 + x_2\bar{\theta})\right\}$ and $\left\{\frac{1}{\sqrt{5}}\alpha(x_3 + x_4\theta), \frac{1}{\sqrt{5}}j\bar{\alpha}(x_3 + x_4\bar{\theta})\right\}$. In this paper, only the pair of GCs $\left\{\frac{1}{\sqrt{5}}\alpha(x_1 + x_2\theta), \frac{1}{\sqrt{5}}\bar{\alpha}(x_1 + x_2\bar{\theta})\right\}$ is used in the proposed N-STBC technique.

III. SYSTEM MODEL

The proposed system model is based on the Alamouti-STBC scheme. In order to enhance the spectral efficiency of the Alamouti-STBC and approximately retain the bit error performance as the conventional Alamouti-STBC, we introduce a dimension (a pair of coupled phase offsets) of order N into one of two transmit antennas, which maps an additional $\log_2 N$ bits into a pair of NPSK STLD symbols per four time-slots, which is refered as N-STBC in this paper.

Consider that the proposed N-STBC system contains $N_t = 2$ transmit antennas and N_r receive antennas. The proposed N-STBC scheme operates as follows: Given $r = \log_2 M$ and $s = \log_2 N$, a $(4r + s)$-tuple message is partitioned into $4r$-tuple vectors $\boldsymbol{m}_i = \begin{bmatrix} m_{i,1} & m_{i,2} & \cdots & m_{i,r} \end{bmatrix}$, $i \in [1:4]$ and an s-tuple vector $\boldsymbol{m} = \begin{bmatrix} m_1 & m_2 & \cdots & m_s \end{bmatrix}$. Let q_i be the decimal index of the input binary vector $\boldsymbol{m}_i$, $i \in [1:4]$, where $q_i \in [1:M]$. The vector $\boldsymbol{m}_i$ is then mapped onto MQAM or MPSK constellation points x^i with $E\{|x^i|^2\} = \varepsilon$, $i \in [1:4]$, in the Argand plane, and $x^i \in \boldsymbol{\chi}_s$. $\boldsymbol{\chi}_s$ is the signal set of MQAM or MPSK with modulation order M. However, only MQAM is considered in this paper. Let p be the decimal index of the input binary vector $\boldsymbol{m}$, where $p \in [1:N]$. The vector $\boldsymbol{m}$ is mapped onto a pair of NPSK STLD constellation points (x^1_p, x^2_p), in the Argand plane. $x^k_p \in \boldsymbol{\chi}_p$, $\boldsymbol{\chi}_p$ is the signal set of NPSK with modulation order N. Obviously we have $E\{|x^k_p|^2\} = 1$, $k \in [1:2]$.

In the following two subsections, the N-STBC systems with and without GCs will be presented, respectively.

A. N-STBC WITHOUT GCs

There are two codeword matrices in the proposed N-STBC technique. Based on the conventional Alamouti encoding, the k^{th} codeword matrix of the proposed N-STBC is given by:

$$\boldsymbol{X}^k = \begin{bmatrix} x^{2k-1} & x^k_p x^{2k} \\ -(x^{2k})^* & x^k_p (x^{2k-1})^* \end{bmatrix}. \tag{3}$$

Let $\boldsymbol{X}^k = \begin{bmatrix} \boldsymbol{x}^1_1 & \boldsymbol{x}^1_2 \end{bmatrix}$ and $x^k_p = e^{j\theta_k}$. Then we have:

$$\langle \boldsymbol{x}^1_1, \boldsymbol{x}^1_2 \rangle = x^{2k-1}(x^k_p x^{2k})^* - (x^{2k})^*(x^k_p (x^{2k-1})^*)^* = 0. \tag{4}$$

and

$$\boldsymbol{X}^k(\boldsymbol{X}^k)^H = \left(|x^{2k-1}|^2 + |x^{2k}|^2\right)\boldsymbol{I}_2 \tag{5}$$

where $\boldsymbol{I}_2$ is a 2×2 identity matrix.

Both (4) and (5) prove that (3) still preserves orthogonality, which retains the simple L-ML detection at the receiver.

It takes two time slots to transmit each $\boldsymbol{X}^k$. In time slot 1, antenna 1 transmits the symbol x^{2k-1}, while antenna 2 transmits the symbol $x_p^k x^{2k}$. In time slot 2, antenna 1 transmits the symbol $-(x^{2k})^*$, while antenna 2 transmits the symbol $x_p^k(x^{2k-1})^*$. The received signals at the receiver are given by:

$$\boldsymbol{y}^{2k-1} = x^{2k-1}\boldsymbol{h}^{2k-1} + x_p^k x^{2k}\boldsymbol{h}^{2k} + \boldsymbol{w}^{2k-1}, \tag{6.1}$$

$$\boldsymbol{y}^{2k} = -(x^{2k})^*\boldsymbol{h}^{2k-1} + x_p^k(x^{2k-1})^*\boldsymbol{h}^{2k} + \boldsymbol{w}^{2k}, \tag{6.2}$$

where $\boldsymbol{y}^l \in \mathbb{C}^{N_r \times 1}$ is the signal vector received at the receiver, $l \in [1:4]$. $\boldsymbol{h}^l \in \mathbb{C}^{N_r \times 1}$ is the channel coefficient vector. Each $\boldsymbol{h}^l$ lasts two time slots, and takes another independent channel coefficient vector in the next two time slots. $\boldsymbol{w}^l \in \mathbb{C}^{N_r \times 1}$ is the additive white Gaussian noise (AWGN) vector. The entries of both $\boldsymbol{h}^l$ and $\boldsymbol{w}^l$ are mutually independent and identically distributed (i.i.d.) complex Gaussian random variables (RVs) distributed as $CN(0, 1)$ and $CN(0, \frac{2\varepsilon}{\rho})$, where ρ is the SNR at each receive antenna.

B. N-STBC WITH GCs

The proposed N-STBC without GCs achieves diversity order $2N_r$. In order to improve error performance at high SNRs, in this paper, we further propose N-STBC with GCs. The proposed N-STBC with GCs achieves diversity order $4N_r$. In order to achieve diversity order $4N_r$ x^{2k} is rotated by $x_p^k, k \in [1:2]$ in the Golden encoding.

There are two encodings in the proposed N-STBC with GCs.

Encoding 1: Golden Encoding.

Based on the pair of GCs $\left\{\frac{1}{\sqrt{5}}\alpha(x_1 + x_2\theta), \frac{1}{\sqrt{5}}\bar{\alpha}(x_1 + x_2\bar{\theta})\right\}$ the Golden encoded symbols are given by:

$$x_g^k = \frac{1}{\sqrt{5}}\alpha(x^{2k-1} + x_p^k x^{2k}\theta), \tag{7.1}$$

$$x_g^{k+2} = \frac{1}{\sqrt{5}}\bar{\alpha}(x^{2k-1} + x_p^k x^{2k}\bar{\theta}), \tag{7.2}$$

where $k \in [1:2]$.

Again, since $E\{|x^i|^2\} = \varepsilon$, then we also have $E\{|x_g^l|^2\} = \varepsilon$, $l \in [1:4]$.

Encoding 2: N-Alamouti Encoding.

Similar to the N-STBC without GCs there are two codeword matrices of the proposed N-STBC with GCs. Based on the conventional Alamouti encoding, the k^{th} codeword matrix of the proposed N-ary Alamouti encoding is given by:

$$\boldsymbol{X}_G^k = \begin{bmatrix} x_g^{2k-1} & x_p^k x_g^{2k} \\ -(x_g^{2k})^* & x_p^k(x_g^{2k-1})^* \end{bmatrix}. \tag{8}$$

Again, (8) also preserves orthogonality, which also makes the L-ML detection feasible at the receiver.

The received signals for N-STBC with GCs are the same as (6.1) and (6.2) by replacing x^l with x_g^l, $l \in [1:4]$.

IV. SIGNAL DETECTION

It is assumed that the channel state information (CSI) is known at the receiver. In the following three subsections, we discuss the signal detection for N-STBC systems with and without GCs, respectively.

A. LINEAR-ML DETECTION FOR N-STBC WITHOUT GCs

The whole signal detection is actually a joint detection of the transmitted pair of coupled phase offsets and the transmitted two symbols. In the following detection algorithm, we calculate the Frobenius distances for all possible pairs of coupled phase offsets. In the N-STBC without GCs, the actual detection includes two steps:

Step 1: Given a pair of coupled phase components (x_p^1, x_p^2) detecting the transmitted symbols, where $x_p^1, x_p^2 \in \boldsymbol{\chi}_p$.

Since both CSI and x_p^k are known at the receiver, we define $\tilde{\boldsymbol{h}}^{2k} = x_p^k\boldsymbol{h}^{2k}$. Then (6.1) and (6.2) are rewritten as:

$$\boldsymbol{y}^{2k-1} = x^{2k-1}\boldsymbol{h}^{2k-1} + x^{2k}\tilde{\boldsymbol{h}}^{2k} + \boldsymbol{w}^{2k-1}, \tag{9.1}$$

$$\boldsymbol{y}^{2k} = -(x^{2k})^*\boldsymbol{h}^{2k-1} + (x^{2k-1})^*\tilde{\boldsymbol{h}}^{2k} + \boldsymbol{w}^{2k}. \tag{9.2}$$

Then (9.1) and (9.2) become the received signals for the conventional Alamouti-STBC scheme. For each pair of NPSK symbols, (x_p^1, x_p^2), $x_p^k \in \boldsymbol{\chi}_p$, $k \in [1:2]$ the combined signals at the receiver may be formulated as follows:

$$z^{2k-1} = [(\boldsymbol{h}^{2k-1})^H\boldsymbol{y}^{2k-1} + (\boldsymbol{y}^{2k})^H\tilde{\boldsymbol{h}}^{2k}], \tag{10.1}$$

$$z^{2k} = [(\tilde{\boldsymbol{h}}^{2k})^H\boldsymbol{y}^{2k-1} - (\boldsymbol{y}^{2k})^H\boldsymbol{h}^{2k-1}]. \tag{10.2}$$

Equivalently, (10.1) and (10.2) may be rewritten as:

$$z^{2k-1} = \beta^k x^{2k-1} + v^{2k-1}, \tag{11.1}$$

$$z^{2k} = \beta^k x^{2k} + v^{2k}, \tag{11.2}$$

where:

$$\beta^k = \|\boldsymbol{h}^{2k-1}\|_F^2 + \|\tilde{\boldsymbol{h}}^{2k}\|_F^2.$$

$$v^{2k-1} = (\boldsymbol{h}^{2k-1})^H\boldsymbol{w}^{2k-1} + (\boldsymbol{w}^{2k})^H\tilde{\boldsymbol{h}}^{2k};$$

$$v^{2k} = (\tilde{\boldsymbol{h}}^{2k})^H\boldsymbol{w}^{2k-1} - (\boldsymbol{w}^{2k})^H\boldsymbol{h}^{2k-1}.$$

Finally, the estimated symbol is given by:

$$\hat{x}^{l,p} = \mathcal{D}\left(\frac{z^l}{\beta^k}\right), \tag{12}$$

where $l \in [1:4]$.

Note (12) denotes that the estimation of the transmitted symbol x^l is $\hat{x}^{l,p}$ given a pair of phase components (x_p^1, x_p^2).

Step 2: Jointly detecting the transmitted signals x^l and (x_p^1, x_p^2).

For convenience of discussion, we define the detected signal vector as $\hat{\boldsymbol{x}}_1^p = (\hat{x}^{1,p}, \hat{x}^{2,p}, \hat{x}^{3,p}, \hat{x}^{4,p})$ for given $\boldsymbol{x}_2^p =$

(x_p^1, x_p^2). Finally, the estimation of the transmitted signals x^l and (x_p^1, x_p^2) is given by:

$$[\hat{\boldsymbol{x}}_1^p, \hat{\boldsymbol{x}}_2^p] = \min_{x_p^1, x_p^2 \in \boldsymbol{\chi}_p} \sum_{k=1}^{4} ED_k, \tag{13}$$

where:

$$\begin{aligned}
ED_1 &= \|\boldsymbol{y}^1 - \hat{x}^{1,p}\boldsymbol{h}^1 - x_p^1 \hat{x}^{2,p}\boldsymbol{h}^2\|_F^2;\\
ED_2 &= \|\boldsymbol{y}^2 + \left(\hat{x}^{2,p}\right)^* \boldsymbol{h}^1 - x_p^1 \left(\hat{x}^{1,p}\right)^* \boldsymbol{h}^2\|_F^2;\\
ED_3 &= \|\boldsymbol{y}^3 - \hat{x}^{3,p}\boldsymbol{h}^3 - x_p^2 \hat{x}^{4,p}\boldsymbol{h}^4\|_F^2;\\
ED_4 &= \|\boldsymbol{y}^4 + \left(\hat{x}^{4,p}\right)^* \boldsymbol{h}^3 - x_p^2 \left(\hat{x}^{3,p}\right)^* \boldsymbol{h}^4\|_F^2.
\end{aligned}$$

B. THE L-ML DETECTION FOR N-STBC WITH GCs

Based on the detection in subsection A the L-ML detection for N-STBC with GCs includes three steps:

Step 1: Given a pair of coupled phase components (x_p^1, x_p^2) detecting the transmitted GCs, where $x_p^1, x_p^2 \in \boldsymbol{\chi}_p$.

Detecting the transmitted GCs is the same as detecting the transmitted symbols in the N-STBC without GCs. Similar to (11.1) and (11.2), we have:

$$r_g^{2k-1} = x_g^{2k-1} + v^{2k-1}/\beta^k, \tag{14.1}$$
$$r_g^{2k} = x_g^{2k} + v^{2k}/\beta^k. \tag{14.2}$$

Step 2: Estimating the transmitted symbols.

Based on $x_g^k = \frac{1}{\sqrt{5}}\alpha(x^{2k-1} + x_p^k x^{2k}\theta)$ and $x_g^{k+2} = \frac{1}{\sqrt{5}}\bar{\alpha}(x^{2k-1} + x_p^k x^{2k}\bar{\theta})$, in (7.1) and (7.2) we can easily obtain:

$$r_x^{2k-1} = \frac{\sqrt{5}}{\mu}\left(\frac{\theta r_g^{k+2}}{\bar{\alpha}} - \frac{\bar{\theta} r_g^k}{\alpha}\right), \tag{15.1}$$
$$r_x^{2k} = \left(x_p^k\right)^* \frac{\sqrt{5}}{\mu}\left(\frac{r_g^k}{\alpha} - \frac{r_g^{k+2}}{\bar{\alpha}}\right), \tag{15.2}$$

where: $\mu = \theta - \bar{\theta}$.

Finally, the estimated symbol is given by:

$$\hat{x}^{l,p} = \mathcal{D}\left(r_x^l\right), \tag{16}$$

where $l \in [1:4]$.

Step 3: Jointly detecting the transmitted signals x^l and (x_p^1, x_p^2).

This step is very similar to Step 2 in N-STBC without GCs. From (16) we obtain the estimated $\hat{x}^{l,p}$. Then we further have estimated GCs $\hat{x}_g^{k,p} = \frac{1}{\sqrt{5}}\alpha(\hat{x}^{2k-1,p} + x_p^k \hat{x}^{2k,p}\theta)$ and $\hat{x}_g^{k+2,p} = \frac{1}{\sqrt{5}}\bar{\alpha}(\hat{x}^{2k-1,p} + x_p^k \hat{x}^{2k,p}\bar{\theta})$. Finally, the estimation of the transmitted signals x^l and (x_p^1, x_p^2) is the same as (13) by replacing $\hat{x}^{l,p}$ with $\hat{x}_g^{l,p}$.

C. SIGNAL DETECTION SUBSET BASED ML DETECTION (SDS-ML) FOR N-STBC WITH GCs

The detection complexity of the above simple L-ML detection for N-STBC with GCs is very low. However, the above simple signal detection cannot achieve the ML performance at high SNRs because (15.1) and (15.2) convert joint detection into individual detection.

SDS-ML detection scheme has been proposed to improve the error performance of the SIMO system with GCs [14]. In this subsection, we also use the SDS-ML detection scheme to improve error performance of the N-STBC with GCs at high SNRs. The only difference between the simple L-ML detection and the SDS-ML detection is that the SDS-ML detection will estimate $\hat{x}^{2k-1,p}$ and $\hat{x}^{2k,p}$ more accurately in Step 2 of the previous subsection. In this subsection, we mainly focus on the estimation of $\hat{x}^{2k-1,p}$ and $\hat{x}^{2k,p}$ using the SDS-ML detection.

The SDS-ML detection is based on the signal detection subset, which is defined as Definition 1.

Definition 1: Let $\boldsymbol{X} = \left(x^1, x^2\right)$ be a pair of MQAM symbols and $\boldsymbol{X}_g = \left(x_g^1, x_g^2\right)$ be a pair of GCs. $\boldsymbol{X}_g$ is constructed by $\boldsymbol{X}$. A signal detection subset of $\boldsymbol{X}_g$ is defined as $\boldsymbol{\chi}(\boldsymbol{X}_g, \delta) = \left\{(x_j^1, x_j^2), \prod_{i=1}^2 |x_j^i - x_g^i|^2 \le \delta, j \in [1 : M^2]\right\}$, where $\delta > 0$.

Compared to the simple L-ML detection in previous subsection, the SDS-ML detection estimates the transmitted symbols more accurately in Step 2.

Based on the estimation of $\hat{x}^{l,p}$ from (16), we can easily obtain $\hat{x}_g^k$ and $\hat{x}_g^{k+2}$ for each pair of symbols $(\hat{x}^{2k-1,p}, \hat{x}^{2k,p})$, further obtain the detection subset $\boldsymbol{\chi}\left(\hat{\boldsymbol{X}}_q, \delta_{\hat{x}}\right)$.

For further detection, (14.1) and (14.2) may be rewritten as:

$$z_g^{2k-1} = \beta^k x_g^{2k-1} + v^{2k-1}, \tag{17.1}$$
$$z_g^{2k} = \beta^k x_g^{2k} + v^{2k}. \tag{17.2}$$

Finally, the SDS-ML detection is given by

$$[\hat{x}_g^1, \hat{x}_g^3] = \underset{\substack{\hat{x}_g^{2k-1} \in \boldsymbol{\chi}(\hat{\boldsymbol{X}}_g, \delta)\\ l \in [1:2]}}{\operatorname{argmin}} \sum_{k=1}^{2} |z_g^{2k-1} - \beta^k \hat{x}_g^{2k-1}|^2, \tag{18.1}$$

$$[\hat{x}_g^2, \hat{x}_g^4] = \underset{\substack{\hat{x}_g^{2k} \in \boldsymbol{\chi}(\hat{\boldsymbol{X}}_g, \delta)\\ l \in [1:2]}}{\operatorname{argmin}} \sum_{k=1}^{2} |z_g^{2k} - \beta^k \hat{x}_g^{2k}|^2. \tag{18.2}$$

Based on $\hat{x}_g^k$ and $\hat{x}_g^{k+2}$ obtained from (18.1) and (18.2), $\hat{x}^{2k-1,p}$ and $\hat{x}^{2k,p}$ will be estimated more accurately.

V. ERROR PERFORMANCE ANALYSIS

In this section, we will derive the error probabilities of the Alamouti-STBC with and without GCs, then prove that the error probabilities of the Alamouti-STBC with and without GCs are the lower error probability bounds of the N-Alamouti-STBC with and without GCs, respectively.

A. ERROR PERFORMANCE OF THE ALAMOUTI-STBC

The N-STBC becomes the conventional Alamouti-STBC when $x_p^k = 1$. Then the equivalently received signal in (11.1)

becomes:

$$z^k = (\|\boldsymbol{h}^1\|_F^2 + \|\boldsymbol{h}^2\|_F^2)x^k + v^k, k \in [1:2], \quad (19)$$

where:

$$v^1 = (\boldsymbol{h}^1)^H \boldsymbol{w}^1 + (\boldsymbol{w}^2)^H \boldsymbol{h}^2;$$
$$v^2 = (\boldsymbol{h}^2)^H \boldsymbol{w}^1 - (\boldsymbol{w}^2)^H \boldsymbol{h}^1.$$

As discussed in Section III, $E\{|x^i|^2\} = \varepsilon$ in (19) and the element of $\boldsymbol{w}^i, i \in [1:2]$ is distributed as $CN(0, \frac{2\varepsilon}{\rho})$. (19) is equivalent to a SIMO system with $2N_r$ receive antennas and $\frac{\rho}{2}$ transmit power, which is well known in the literature.

Based on the exact symbol error probability of MQAM in Equ. (8.10) in [18], and the approximated expression of the Gaussian Q-function using the trapezoidal rule, the average bit error probability (ABEP) of the above MQAM SIMO system with $2N_r$ receive antennas and $\frac{\rho}{2}$ transmit power may be derived as:

$$p_e = \frac{a}{n\log_2 M}\Big[B_1 - B_2 + B_3 + B_4\Big], \quad (20)$$

where:

$$B_1 = \frac{1}{2}\left(\frac{2}{2+b\bar{\gamma}}\right)^{2N_r};$$
$$B_2 = \left(\frac{a}{2}\right) \times \left(\frac{1}{1+b\bar{\gamma}}\right)^{2N_r};$$
$$B_3 = (1-a)\sum_{i=1}^{n-1}\left(\frac{u_i}{u_i+\bar{\gamma}}\right)^{2N_r};$$
$$B_4 = \sum_{i=n}^{2n-1}\left(\frac{u_i}{u_i+b\bar{\gamma}}\right)^{2N_r}.$$

In (20), $n \geq 6$ is the number of summations for convergence, $\bar{\gamma} = \frac{\rho}{2\varepsilon}$, $a = 1 - \frac{1}{\sqrt{M}}$, $b = \frac{3}{M-1}$, and $u_i = 2\sin^2(\frac{i\pi}{4n})$.

B. ERROR PERFORMANCE OF THE ALAMOUTI-STBC WITH GCs

The N-STBC with GCs becomes the conventional Alamouti-STBC with GCs when $x_p^k = 1$. Then the equivalently received signals in (14.1) and (14.2) become:

$$z_g^{2k-1} = \beta^k r_g^{2k-1} = \beta^k x_g^{2k-1} + v^{2k-1}, \quad (21.1)$$
$$z_g^{2k} = \beta^k r_g^{2k} = \beta^k x_g^{2k} + v^{2k}, \quad (21.2)$$

where $\beta^k = \|\boldsymbol{h}^{2k-1}\|_F^2 + \|\boldsymbol{h}^{2k}\|_F^2$.

Furthermore, as an example, the equivalently received signals for detecting a pair of GCs (x_g^1, x_g^3) become:

$$z_g^1 = \beta^1 x_g^1 + v^1, \quad (22.1)$$
$$z_g^3 = \beta^2 x_g^3 + v^3. \quad (22.2)$$

From the equivalently received signals, it is easily seen that the orthogonality of the Alamouti-STBC converts the MIMO system into SIMO systems. Since $x_g^1 = \frac{1}{\sqrt{5}}\alpha(x^1 + x^2\theta)$ and $x_g^3 = \frac{1}{\sqrt{5}}\bar{\alpha}(x^1 + x^2\bar{\theta})$, both x_g^1 and x_g^3 convey the same information. Thus we can regard both x_g^1 and x_g^3 are transmitted in non-identical fading channels in a SIMO system. The error performance of the SIMO system with GCs has been derived in [14]. The ABEP of the SIMO system with GCs derived in (5) of [14] is given by:

$$P_e(\rho) \leq \frac{1}{2M^2 r}\sum_{g=1}^{M^2}\sum_{\hat{g}\neq g}^{M^2} N(g,\hat{g})P\big(\boldsymbol{X}_g \to \boldsymbol{X}_{\hat{g}}\big), \quad (23)$$

where $r = \log_2 M$. $\boldsymbol{X}_g = \big(x_g^1\ x_g^3\big)$ and $\boldsymbol{X}_{\hat{g}} = \big(x_{\hat{g}}^1\ x_{\hat{g}}^3\big)$. $N(g,\hat{g})$ is the number of bit errors for the associated pairwise error probability (PEP) event. $P\big(\boldsymbol{X}_g \to \boldsymbol{X}_{\hat{g}}\big)$ is the PEP that the transmitted GC $\boldsymbol{X}_g$ is detected as $\boldsymbol{X}_{\hat{g}}$ at the receiver. In [14], the PEP of the SIMO with GCs is given by:

$$P\big(\boldsymbol{X}_q \to \boldsymbol{X}_{\hat{q}}\big) = \frac{1}{4n}\Big[A_1 + A_2\Big], \quad (24)$$

where:

$$A_1 = \frac{1}{2}\prod_{i=1}^{2}\left(1 + \frac{\rho}{4\varepsilon}|d_x^i|^2\right)^{-N_r};$$
$$A_2 = \sum_{k=1}^{n-1}\prod_{i=1}^{2}\left(1 + \frac{\rho}{4\varepsilon}|d_x^i|^2\frac{1}{u_k}\right)^{-N_r}.$$

In the derivation of (24), the trapezoidal approximation of the Gaussian Q-function is applied for integration. n in (24) is the same as the meaning of n in (20). $u_k = \sin^2\left(\frac{k\pi}{2n}\right)$ and $d_x^i = x_p^i - x_{\hat{p}}^i, i \in [1:2]$.

The average ABEP for the Alamouti-STBC with GCs can be easily derived by replacing N_r with $2N_r$ and replacing ρ with $\frac{\rho}{2}$ in (24).

C. LOWER ERROR PROBABILITY BOUND OF THE N-STBC WITHOUT GCs

In this subsection, we derive the lower error probability bound of the N-STBC without GCs.

In the N-STBC without GCs, let $x_p^k = e^{j\theta_k}$ in (6.1) and (6.2). Then we have:

$$\boldsymbol{y}^{2k-1} = x^{2k-1}\boldsymbol{h}^{2k-1} + e^{j\theta_k}x^{2k}\boldsymbol{h}^{2k} + \boldsymbol{w}^{2k-1}, \quad (25.1)$$
$$\boldsymbol{y}^{2k} = -(x^{2k})^*\boldsymbol{h}^{2k-1} + e^{j\theta_k}(x^{2k-1})^*\boldsymbol{h}^{2k} + \boldsymbol{w}^{2k}. \quad (25.2)$$

We can treat $e^{j\theta_k}$ as an interference. Let $e^{j\theta_k}x^{2k} = x^{2k} + \delta_1$ and $e^{j\theta_k}(x^{2k-1})^* = (x^{2k-1})^* + \delta_2$. Then (25.1) and (25.2) become:

$$\boldsymbol{y}^{2k-1} = x^{2k-1}\boldsymbol{h}^{2k-1} + x^{2k}\boldsymbol{h}^{2k} + \tilde{\boldsymbol{w}}^{2k-1}, \quad (26.1)$$
$$\boldsymbol{y}^{2k} = -(x^{2k})^*\boldsymbol{h}^{2k-1} + (x^{2k-1})^*\boldsymbol{h}^{2k} + \tilde{\boldsymbol{w}}^{2k}, \quad (26.2)$$

where:

$$\tilde{\boldsymbol{w}}^{2k-1} = \delta_1\boldsymbol{h}^{2k} + \boldsymbol{w}^{2k-1};$$
$$\tilde{\boldsymbol{w}}^{2k} = \delta_2\boldsymbol{h}^{2k} + \boldsymbol{w}^{2k}.$$

It is assumed that the CSI is known at the receiver. Since both δ_1 and δ_2 are RVs, both $\delta_1\boldsymbol{h}^{2k}$ and $\delta_2\boldsymbol{h}^{2k}$ are also RVs, which are regarded as extra noises. So based on (26.1) and (26.2), the error probability of the conventional Alamouti scheme is the lower error probability bound of N-STBC without GCs.

Similarly, we can also easily derive that the error probability of the Alamouti scheme with GCs is the lower error probability bound of the N-STBC with GCs.

VI. NUMERICAL RESULTS

In this section, we present the simulation results for the proposed N-STBC with and without GCs. In the simulations, it is assumed that the CSI is fully known at the receiver. It is also assumed that the channel fading coefficients $\boldsymbol{h}_i, i \in [1:4]$ with AWGN are the same as discussed in Section III. The constellation mappers for STLD with 16PSK is given in TABLE 1. The constellation mappers for STLD with other MPSK are given in Appendix A. In the SDS-ML detection, δ is set to be 16. For comparison, we also calculate the theoretical results of (20) and (23) and validate these theoretical results as lower error probability bounds for N-STBC with and without GCs by simulations. In all figures, the legends $2 \times N_r$ MQAM N-STBC L-ML and $2 \times N_r$ MQAM STBC bound, denote the simulated bit error rate (BER) using L-ML detection and the lower error probability bound for $2 \times N_r$ N-STBC without GCs. 1-STBC denotes the Alamouti-STBC. The legends, $2 \times N_r$ MGQAM N-STBC L-ML, $2 \times N_r$ MGQAM N-STBC SDS-ML and $2 \times N_r$ MGQAM-STBC bound, denote the simulated BER using L-ML, simulated BER using SDS-ML and the lower error probability bound for $2 \times N_r$ N-STBC with GCs.

A. LOWER ERROR PROBABILITY BOUND FOR N-STBC WITH AND WITHOUT GCs

In this subsection, we simulated 2×2 16QAM and 64QAM N-STBC with and without GCs. The simulated BERs and the theoretical bounds of (20) and (23) are shown in Figs. 1 and 2. From Fig. 1 it is observed that the lower error probability bounds well predict the BER at high SNRs for both 16QAM and 64QAM for 16-STBC without GCs. From Fig. 2 it is observed that the lower error probability bounds well predict the BER at high SNRs for both 16GQAM for 8-STBC and 64GQAM for 16-STBC with GCs.

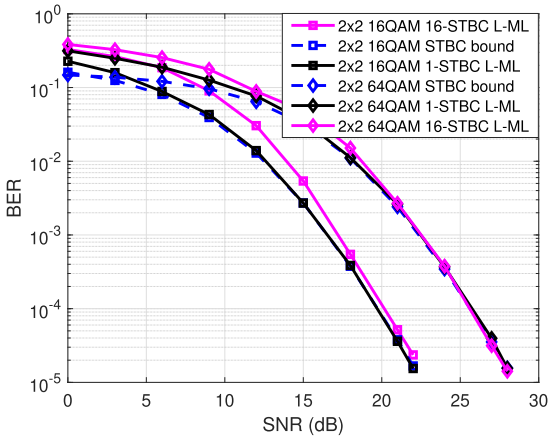

FIGURE 1. BER and bound for 2 × 2 16QAM and 64QAM 16-STBC without GCs.

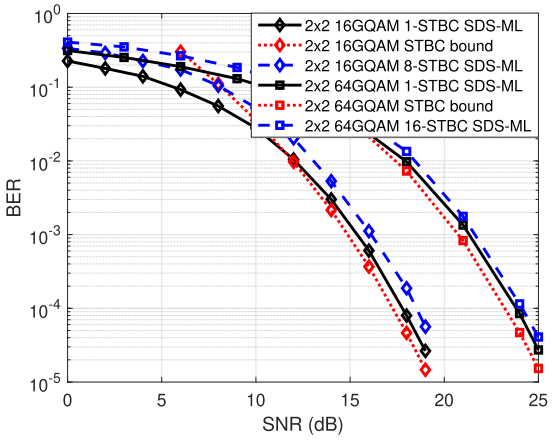

FIGURE 2. BER and bound for 2 × 2 16QAM 8-STBC and 64QAM 16-STBC with GCs.

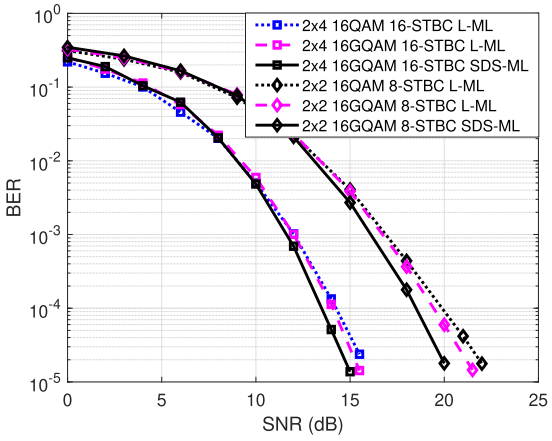

FIGURE 3. BER comparison between L-ML and SDS-ML 2 × 2 and 2 × 4 16QAM 16-STBC with GCs.

B. L-ML VS SDS-ML FOR N-STBC WITH GCs

In this subsection, we compared the error performance between the L-ML and the SDS-ML for N-STBC with GCs. The simulated BERs are shown in Figs. 3 and 4 for 2×2, 2×4 8-STBC and 16-STBC with GCs, respectively.

From Figs. 3 and 4, it is observed that 16-STBC with GCs using L-ML improved error performance compared to 16-STBC without GCs. Similarly it is also observed that 16-STBC with GCs using SDS-ML improved error performance compared to 16-STBC with GCs using L-ML. However, as the number of receive antennas increases, the SNR gain achieved by the SDS-ML is becoming smaller compared to the L-ML.

C. NPSK VS THE NUMBER OF RECEIVE ANTENNAS

In the proposed N-STBC with and without GCs, the number of receive antennas N_r determines the PSK modulation order N. In this subsection, we discuss how N_r affects PSK modulation order N. We only simulated 2×2 and 2×4 16QAM N-STBC with and without GCs. The simulated BER results are shown in Figs. 5 and 6. From Fig. 5 it is observed that 4-STBC achieves the error performance of 1-STBC for

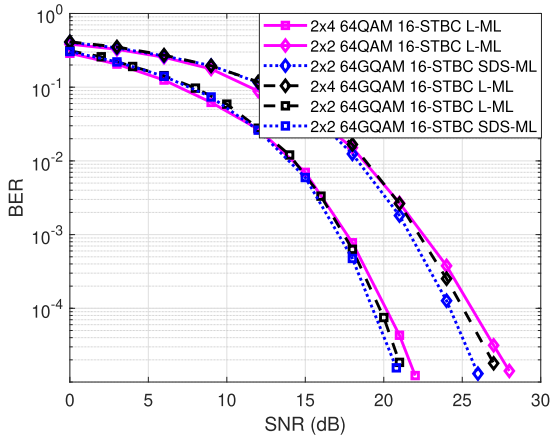

FIGURE 4. BER comparison between L-ML and SDS-ML 2 × 2 and 2 × 4 64QAM 16-STBC with GCs.

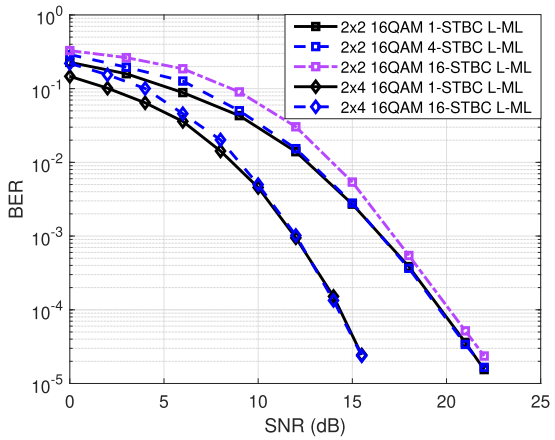

FIGURE 5. *N*PSK vs N_r for 16QAM *N*-STBC without GCs.

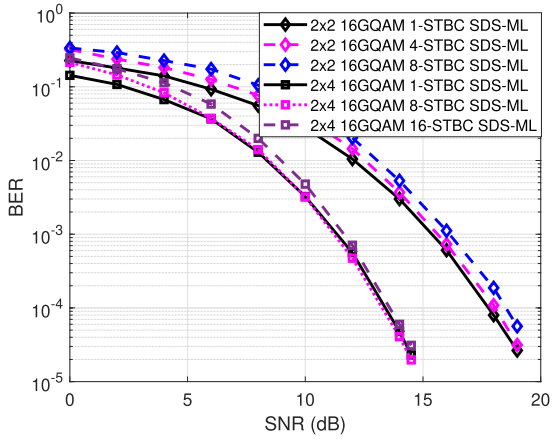

FIGURE 6. *N*PSK vs N_r for 16QAM *N*-STBC with GCs.

2 × 2 STBC without GCs, while 16-STBC achieves the error performance of 1-STBC for 2×4 STBC without GCs. Similar observation is found in Fig. 6 for N-STBC with GCs. So the value of N increases as N_r increases to achieve the error performance of 1-STBC with and without GCs.

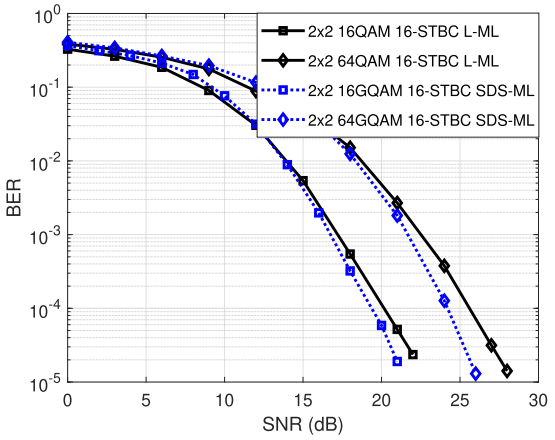

FIGURE 7. BER comparison for 2 × 2 16QAM and 64QAM 16-STBC with and without GCs.

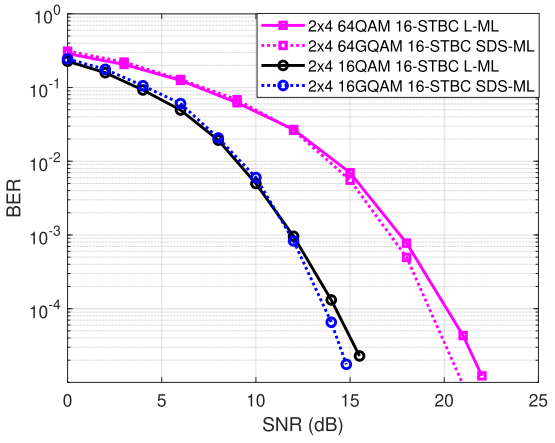

FIGURE 8. BER comparison for 2 × 4 16QAM and 64QAM 16-STBC with and without GCs.

D. THE N-STBC WITH GCS VS THE N-STBC WITHOUT GCs

In this subsection, we compare the error performance of the N-STBC systems between with and without GCs. The simulated BERs for 2 × 2 and 2 × 4 16QAM and 64QAM 16-STBC with and without GCs are shown in Figs. 7 and 8, respectively. From Figs. 7 and 8 it is observed that 16-STBC with GCs outperforms 16-STBC without GCs at least 0.8 dB and 1.5 dB for 16QAM and 64QAM at the BER of 2×10^{-5}. The SNR gain achieved by the N-STBC with GCs increases as M increases. This is because N-STBC with GCs achieves diversity order $4N_r$, while N-STBC without GCs only achieves diversity order $2N_r$.

VII. CONCLUSION

In this paper, we proposed a novel N-STBC technique to convey information in MIMO systems. In the proposed N-STBC technique, the extra information is conveyed by one channel's phase component. The N-STBC with GCs is further proposed to improve error performance compared to the N-STBC without GCs at high SNRs. We also discussed the L-ML detection in the N-STBC with GCs. Moreover, we discussed both L-ML and SDS-ML for the N-STBC

without GCs. We also derived the lower error probability bounds of the N-STBC with and without GCs. Finally, the simulation results demonstrate that the proposed N-STBC with and without GCs almost maintain the error performance of 1-STBC with and without GCs at high SNRs.

APPENDIX A

TABLE 2. Constellation mappers for 8PSK.

q	0	1	2	3	4	5	6	7
Ω_8^1	θ_0	θ_1	θ_3	θ_2	θ_7	θ_6	θ_4	θ_5
Ω_8^2	θ_0	θ_5	θ_7	θ_2	θ_3	θ_6	θ_4	θ_1

TABLE 3. Constellation mappers for 32PSK.

q	0	1	2	3	4	5	6	7
Ω_{32}^1	θ_0	θ_1	θ_3	θ_2	θ_7	θ_6	θ_4	θ_5
Ω_{32}^2	θ_{16}	θ_5	θ_{19}	θ_{23}	θ_{30}	θ_9	θ_{28}	θ_1
q	8	9	10	11	12	13	14	15
Ω_{32}^1	θ_{15}	θ_{14}	θ_{12}	θ_{13}	θ_8	θ_9	θ_{11}	θ_{10}
Ω_{32}^2	θ_7	θ_{14}	θ_{12}	θ_5	θ_8	θ_1	θ_3	θ_{10}
q	16	17	18	19	20	21	22	23
Ω_{32}^1	θ_{31}	θ_{30}	θ_{28}	θ_{29}	θ_{24}	θ_{25}	θ_{27}	θ_{26}
Ω_{32}^2	θ_7	θ_{14}	θ_{12}	θ_5	θ_8	θ_1	θ_3	θ_{10}
q	24	25	26	27	28	29	30	31
Ω_{32}^1	θ_{16}	θ_{17}	θ_{19}	θ_{18}	θ_{23}	θ_{22}	θ_{20}	θ_{21}
Ω_{32}^2	θ_7	θ_{14}	θ_{12}	θ_5	θ_8	θ_1	θ_3	θ_{10}

REFERENCES

[1] V. W. S. Wong, R. Schober, D. W. K. Ng, and L. Wang, *Key Technologies for 5G Wireless Systems*. Cambridge, U.K.: Cambridge Univ. Press, Mar. 2017.
[2] S. M. Alamouti, "A simple transmit diversity technique for wireless communications," *IEEE J. Sel. Areas Commun.*, vol. 16, no. 8, pp. 1451–1458, Oct. 1998.
[3] V. Tarokh, H. Jafarkhani, and A. R. Calderbank, "Space-time block coding for wireless communications: Performance results," *IEEE J. Sel. Areas Commun.*, vol. 17, no. 3, pp. 451–460, Mar. 1999.
[4] V. Tarokh, H. Jafarkhani, and A. R. Calderbank, "Space-time block codes from orthogonal designs," *IEEE Trans. Inf. Theory*, vol. 45, no. 5, pp. 1456–1467, Jul. 1999.
[5] Q. Ling and T. Li, "Efficiency improvement for Alamouti codes," in *Proc. 40th Annu. Conf. Inf. Sci. Syst.*, Mar. 2006, pp. 569–572.
[6] R. Vishwanath and M. R. Bhatnagar, "High data rate Alamouti code from field extension," *Wireless Pers. Commun.*, vol. 40, no. 4, pp. 489–494, Jan. 2007.
[7] S. Das, N. Al-Dhahir, and R. Calderbank, "Novel full-diversity high-rate STBC for 2 and 4 transmit antennas," *IEEE Commun. Lett.*, vol. 10, no. 3, pp. 171–173, Mar. 2006.
[8] M. O. Sinnokrot, J. R. Barry, and V. K. Madisetti, "Embedded Alamouti space-time codes for high rate and low decoding complexity," in *Proc. 42nd Asilomar Conf. Signals, Syst. Comput.*, Oct. 2008, pp. 1749–1753.
[9] E. Basar, U. Aygölü, E. Panayirci, and H. V. Poor, "Space-time block coded spatial modulation," *IEEE Trans. Commun.*, vol. 59, no. 3, pp. 823–832, Mar. 2011.
[10] X. Li and L. Wang, "High rate space-time block coded spatial modulation with cyclic structure," *IEEE Commun. Lett.*, vol. 18, no. 4, pp. 532–535, Apr. 2014.
[11] A. G. Helmy, M. Di Renzo, and N. Al-Dhahir, "Enhanced-reliability cyclic generalized spatial-and-temporal modulation," *IEEE Commun. Lett.*, vol. 20, no. 12, pp. 2374–2377, Dec. 2016.
[12] H. Xu, K. Govindasamy, and N. Pillay, "Uncoded space-time labeling diversity," *IEEE Commun. Lett.*, vol. 20, no. 8, pp. 1511–1514, Aug. 2016.
[13] J. Jeganathan, A. Ghrayeb, L. Szczecinski, and A. Ceron, "Space shift keying modulation for MIMO channels," *IEEE Trans. Wireless Commun.*, vol. 8, no. 7, pp. 3692–3703, Jul. 2009.
[14] H. Xu and N. Pillay, "Golden codeword–based modulation schemes for single-input multiple-output systems," *Int. J. Commun. Syst.*, vol. 32, no. 10, pp. 1–12, Jul. 2019.
[15] N. Pillay and H. Xu, "Reconfigurable intelligent surface-aided single-input single-output K-complex symbol golden codeword based modulation," *IEEE Access*, vol. 9, pp. 71849–71855, 2021.
[16] H. Xu, N. Pillay, and F. Yang, "Rotated golden codewords based space-time line code systems," *IEEE Access*, vol. 10, pp. 54784–54793, 2022.
[17] J.-C. Belfiore, G. Rekaya, and E. Viterbo, "The golden code: A 2×2 full-rate space-time code with non-vanishing determinants," *IEEE Trans. Inf. Theory*, vol. 51, no. 4, pp. 1432–1436, Apr. 2005.
[18] M. K. Simon and M.-S. Alouini, *Digital Communication Over Fading Channels: A Unified Approach to Performance Analysis*. Hoboken, NJ, USA: Wiley, 2000.

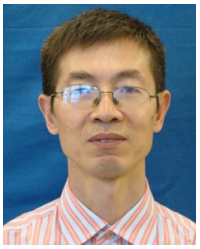

HONGJUN XU (Member, IEEE) received the B.Sc. degree from the Guilin University of Electronic Technology, China, in 1984, the M.Sc. degree from the Institute of Telecontrol and Telemeasure, China, in 1989, and the Ph.D. degree from the Beijing University of Aeronautics and Astronautics, Beijing, China, in 1995. From 1997 to 2000, he was a Postdoctoral Researcher with the University of Natal and Inha University. He is currently a Full Professor with the School of Engineering, University of KwaZulu-Natal, Howard College Campus. He has published more than 50 journal articles. His research interests include digital and wireless communications and digital systems. He is a National Research Foundation (NRF) Rated Researcher in South Africa.

NARUSHAN PILLAY received the M.Sc.Eng. (cum laude) and Ph.D. degrees in wireless communications from the University of KwaZulu-Natal, Durban, South Africa, in 2008 and 2012, respectively. Since 2009, he has been with the University of KwaZulu-Natal. Previously, he was with the Council of Scientific and Industrial Research (CSIR), Defence, Peace, Safety and Security (DPSS), South Africa. He supervised several M.Sc.Eng. and Ph.D. students. His research interests include physical wireless communications, including spectrum sensing for cognitive radio and MIMO systems. He has published several papers in well-known journals in the area of research. He is a National Research Foundation (NRF) Rated Researcher in South Africa.

FENGFAN YANG received the B.Sc. degree in electronic engineering from the Nanjing University of Aeronautics and Astronautics (NUAA), Nanjing, China, in 1990, the M.Sc. degree in electronic engineering from Northwestern Polytechnical University, Xi'an, China, in 1993, and the Ph.D. degree in electronic engineering from Southeast University, Nanjing, in 1997. Since May 1997, he has been with the College of Information Science and Technology, NUAA. From October 1999 to May 2003, he was a Research Associate with the Centre for Communication Systems Research, University of Surrey, Guildford, U.K., and the Department of Electrical and Computer Engineering, McGill University, Montreal, QC, Canada. His major research interests include information theory and channel coding, especially at iteratively decodable codes, such as turbo codes and LDPC codes, and their applications for mobile and satellite communications.